Cancer Imaging (2010) **10,** 183–193
DOI: 10.1102/1470-7330.2010.0025

CI

e-med
www.e-med.org.uk

REVIEW

Treatment monitoring of paranasal sinus tumors by magnetic resonance imaging

Davide Farina, Andrea Borghesi, Elisa Botturi, Marco Ravanelli and Roberto Maroldi

Department of Radiology, Università degli Studi, Brescia, 25123, Italy

Corresponding address: Davide Farina, Department of Radiology, Università degli Studi, Brescia, 25123, Italy.
Email: nappaje@yahoo.it

Date accepted for publication 9 July 2010

Abstract

Treatment monitoring of paranasal tumors is crucial, given the high rate of local and regional relapses that impairs the overall prognosis of patients. Magnetic resonance imaging (MRI) is the technique of choice to detect changes in the submucosa and deep spaces of the suprahyoid neck, inaccessible at clinical and endoscopic assessment. Correct interpretation of MRI requires detailed knowledge of the treatment applied and of the changes treatments are supposed to produce on macroscopic anatomy and tissue signals. Once such background of information is obtained, detection of recurrences is a less challenging task.

Keywords: *Paranasal sinus neoplasm; MRI; diffusion-weighted imaging.*

Introduction

Sinonasal malignancies are rare, accounting for 3% of all head and neck neoplasms. Although a wide range of histotypes, and as a consequence a wide spectrum of diverse pathologies, may be found, the overall prognosis is poor. This is mostly due to local recurrence (which is seen in as many as 50% of patients), even though regional and distant failures cannot be neglected[1,2]; timing of recurrences varies amongst the various histotypes: squamous cell and undifferentiated carcinoma tend to relapse within 2–3 years from treatment, whereas adenocarcinoma, adenoid cystic carcinoma and esthesioneuroblastoma may recur at a steady rate for up to 10–15 years[3,4]. These issues enhance the need for careful and prolonged follow-up, aimed at detecting recurrences when still amenable to salvage treatments. In principle, surgery of sinonasal malignancies leaves large cavities easily accessible at endoscopy. As recurrent tumors frequently do not provoke signs and symptoms in early phases, magnetic resonance imaging (MRI) is required to add information on what happens deep to the mucosa, mainly surveying the orbit, anterior and middle skull base, pterygopalatine fossa and masticator space. The key to the interpretation of follow-up examinations is the detailed knowledge of the type of treatment applied (i.e. the amount of surgical demolition and the strategy for reconstruction) and of the changes they are supposed to produce on MRI images. This article provides a practical approach to imaging follow-up of patients affected by paranasal sinus tumors, by schematically reviewing treatment options, MRI acquisition protocols, normal post-treatment changes and findings in recurrent tumors.

Treatment options

Surgery is the mainstay of treatment for sinonasal neoplasms. According to the site of origin and extension of the primary, basically six different types of resection can be applied (even in combination): inferior, medial and total maxillectomy, orbital exenteration, infratemporal fossa resection and craniofacial resection[5]. Since the 1960s, craniofacial resection is regarded as the gold standard technique for ethmoid tumors involving the anterior skull base[6]. In recent years, the transnasal approach has also been proposed, both for purely endoscopic and for cranioendoscopic resection of well-selected malignant sinonasal neoplasms[7,8]. This technique is supposed to decrease the significant complication and mortality rates (36% and 4.7%, respectively) of craniofacial resection, yet the oncologic results require confirmation in long-term

follow-up studies[4,9]. Crucial to the understanding of postoperative examinations, extensive resections require sometimes complex reconstructions, particularly to restore the separation between nasal cavities and the anterior skull base. Traditional open craniotomic access allows a range of reconstructive techniques to be used, including pericranial flaps, split thickness bone flaps, dural substitutes and temporalis muscle flaps[10,11]. The latter are also utilized to fill the gaps created by orbital exenteration or extensive resections of the maxilla. Endoscopic repair of the anterior skull base is obtained through a sandwich of layers made up of synthetic dural substitutes plus two fascial grafts, one extradural intracranial and the other extracranial; fat grafts covered by cellulose material can then be placed to complete the sealing[8–10]. Adjuvant radiation therapy (and chemotherapy) is most commonly administered after surgery, particularly in locally advanced lesions (T3–T4)[12]; in unresectable lesions[3,12], radiotherapy was also suggested as a definitive modality for sinonasal squamous cell and undifferentiated carcinomas.

MRI technique

MRI is generally regarded as the technique of choice for morphologic imaging after sinonasal surgery of malignant neoplasms because of its superb contrast resolution, particularly valuable for the assessment of crucial areas such as the anterior skull base, the pterygopalatine fossa, the foramina and fissures that connect it to the orbit and middle cranial fossa. The standard protocol (Table 1) requires the use of a head coil and is composed of turbo spin echo (TSE) T2, spin echo (SE) T1 and three-dimensional (3D) gradient echo (GE) fat-saturated sequences; as a rule of thumb, at least one sequence in every different plane should be acquired, in particular sagittal images should never be neglected after anterior skull base reconstruction. The parameters of all sequences are set to provide high resolution while maintaining high signal to noise ratio. In SE sequences, for example, 3-mm slice thickness, 210-mm field-of-view and 208×512 matrix size result in a voxel size of $0.8 \times 0.4 \times 3$ mm. This is an optimal compromise: smaller voxels, such as for slices thinner than 3 mm, will excessively decrease the signal-to-noise ratio; in contrast, larger voxels are unfit for the assessment of the skull base and its foramina and fissures. 3D GE fat-suppressed sequences are extremely helpful, as they combine excellent spatial resolution (isotropic voxel size as small as 0.5 mm) and high contrast resolution (due to fat suppression). Although longer than for SE, acquisition time is still reasonable as motion artifacts are a less significant issue in the sinonasal area than in other head and neck regions. In principle, the MRI protocol may be refined by adding dynamic contrast-enhanced (DCE) and diffusion-weighted sequences (DWI) (Table 2). DCE is obtained acquiring T1-weighted GE sequences with high temporal resolution (4–8s) before and during the administration of contrast agent. These image sets can be used to plot enhancement versus time curves of pathologic and reference normal tissues as well as to extract pharmacokinetic parameters exploring vessel permeability, leakage space fraction, etc.[13]. The former semiquantitative approach is expected to discriminate recurrent tumor from scar tissue[14,15], while the latter quantitative one is more focused on short-term follow-up, namely on the stratification of patient responders to chemoradiation therapy schemes[16]. DWI sequences depict and measure (through apparent diffusion coefficient (ADC) values) the motion (i.e. diffusion) of water protons in tissues. Essentially, diffusion is supposed to be restricted in tumors (thus resulting in a hyper signal and low ADC values) compared with normal or edematous tissues (displaying a low signal and high ADC values). In the head and neck area, DWI is technically demanding because the inhomogeneity of the main magnetic field at the air/bone interface produces distortion of the anatomy and ghosting artifacts, particularly on echo

Table 1 Standard MRI sequences

Sequence	Repetition time (TR) (ms)	Echo time (TE) (ms)	Slice thickness (mm)	Average	Matrix	Voxel (mm)	Acquisition time
TSE T2	5730	126	3	3	208×512	$0.4 \times 0.8 \times 3$	1 min 50 s
SE T1	400	15	3	2	208×512	$0.4 \times 0.8 \times 3$	2 min 50 s
3D GE fat suppressed	8.20	3.16	0.5	1	322×448	$0.5 \times 0.5 \times 0.5$	3 min 49 s

Table 2 Additional MRI sequences

Sequence	Repetition time (TR) (ms)	Echo time (TE) (ms)	Slice thickness (mm)	Matrix	No. of measurements	b-factor	Acquisition time
DCE[a]	8.07	2.76	3	224×179	25	–	2 min 58 s
EPI-DWI	3000	87	3	128×128	–	0–1000	1 min 15 s

[a]Dynamic acquisitions are preceded by multiple flip angle acquisitions in order to calculate a baseline T1 map.

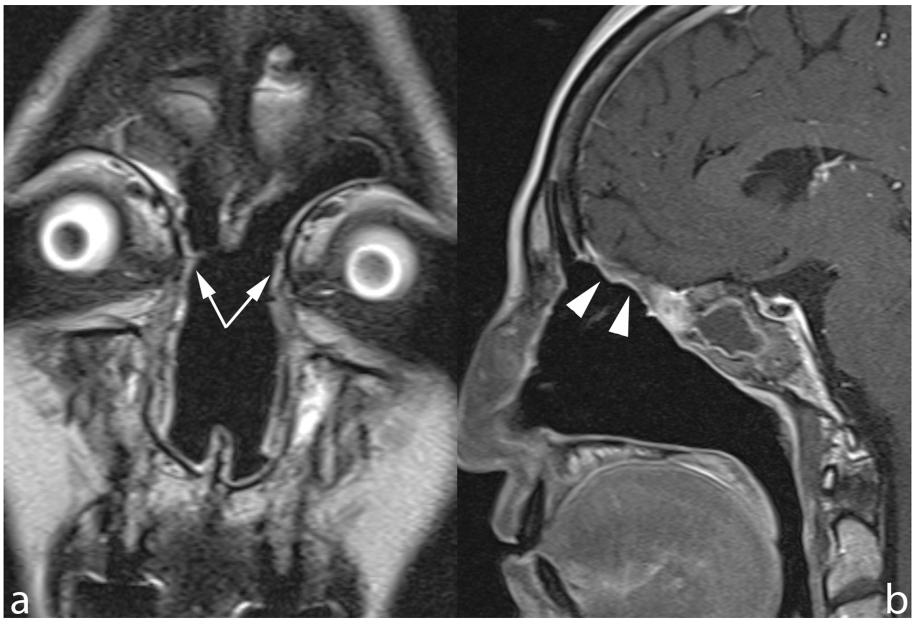

Figure 1 **Microendoscopic ethmoidectomy and frontal sinusotomy (Draf-III approach). Coronal TSE T2 (a) and sagittal contrast enhanced SE T1 (b) show the wide communication created between frontal sinuses and nasal fossa (arrows). The duraplasty (arrowheads) exhibits a regular profile, the sphenoid sinus is occupied by thickened mucosa and retained secretions.**

planar imaging (EPI) sequences. This issue can be addressed using parallel imaging and all the tricks reducing echo time (bandwidth increase, use of monopolar gradients, etc.) or by acquiring single-shot TSE-DWI sequences, which decrease artifacts applying a 180° radiofrequency (RF) refocusing pulse[17]. Beyond feasibility, the clinical application is far from being established; in a group of diverse head and neck tumors, Abdel-Razek *et al.*[18] demonstrated a significant difference between ADC values of recurrent tumors and post-treatment changes, although substantial overlapping was found. Furthermore, the lack standardization of ADC values (mainly due to the use of different sequences and different gradient-shape design by the manufacturers) still suggests caution in the routine application of the technique.

Normal postoperative MRI findings and recurrences

Normal postoperative MRI appearance is the result of a combination of three factors: extension of the resection, type of reconstruction and treatment related inflammatory findings, which highlight the need to obtain a detailed clinical report prior to scanning.

Extension of the resection

Wide resections of the bony sinonasal framework may significantly alter the anatomy: the Draf-III microendoscopic approach to the frontal sinus[19], for example, entails resection of the upper part of the nasal septum and frontal intersinus septum along with drilling of the floor of the frontal sinuses (Fig. 1). Complete removal of the medial orbital wall may induce collapse of extraconal fat within the nasal fossa with enophthalmos (Fig. 2); in addition, extended maxillectomy including

Figure 2 **Follow-up scan after ethmoidectomy and craniofacial resection. Contrast-enhanced SE T1 on axial plane shows prolapse of orbital fat (arrows) into the residual nasal fossa, secondary to complete removal of the medial wall of the right orbit.**

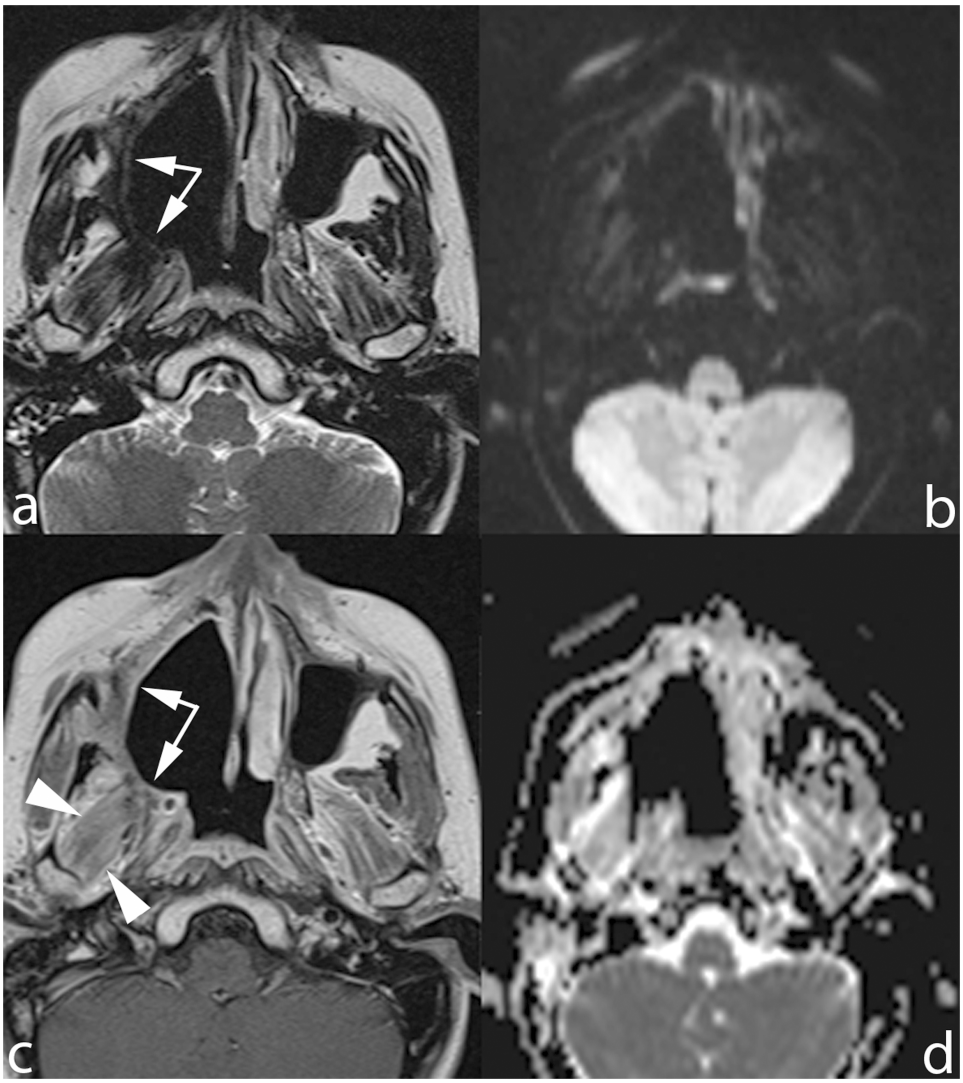

Figure 3 **Early follow-up scan obtained after radical maxillectomy extended to the right hemipalate. The surgical cavity is delimited by a thick plaque of solid tissue (arrows) hypointense on TSE T2 (a) and mildly hyperintense on contrast-enhanced SE T1 MRI (b). This tissue is neither hyperintense DWI b-1000 (c) nor restricting on ADC map (d), thus consistent with fibrotic scar. Diffuse enhancement of lateral pterygoid muscle, secondary to post-RT inflammation (arrowheads).**

the posterolateral sinus wall induces large scars in the adjacent deep soft tissues (infratemporal fossa and masticator space). These are shown on MRI as T2 hypointense plaques with fairly regular thickness; enhancement is variable, faint or absent in long-term follow-up studies, often very strong in the early stages. In these cases, DWI imaging may be of help. In our unpublished experience on 131 patients followed up for squamous cell carcinoma of the head and neck, the 40 recurrences appeared bright on b-1000 images, the mean ADC value of recurrences was comparable with that of primary tumors (0.97×10^{-3} mm^2/s vs $0.89 \times 10^{-3}\,mm^2/s$, $p = ns$); conversely, mature scar lesions invariably appeared dark as background normal tissues on b1000 images (Fig. 3).

Type of reconstruction

Two paradigms may be used to discuss the change produced by surgical reconstructions, namely skull base reconstruction and muscular flap harvesting. In open surgery, skull base reconstruction is accomplished by the meningogaleal complex, a sandwich of layers composed of lyophilized dura or autologous fascia lata and a flap of calvarial pericranium (Fig. 4). A three-layered technique, obtained by harvesting an iliotibial flap, has been described for reconstruction during microendoscopic surgery. On TSE T2 sequences the reconstructed skull base generally exhibits a hypointense signal and contrast enhancement is variable. Discrimination between the different layers of these sandwiches is beyond the

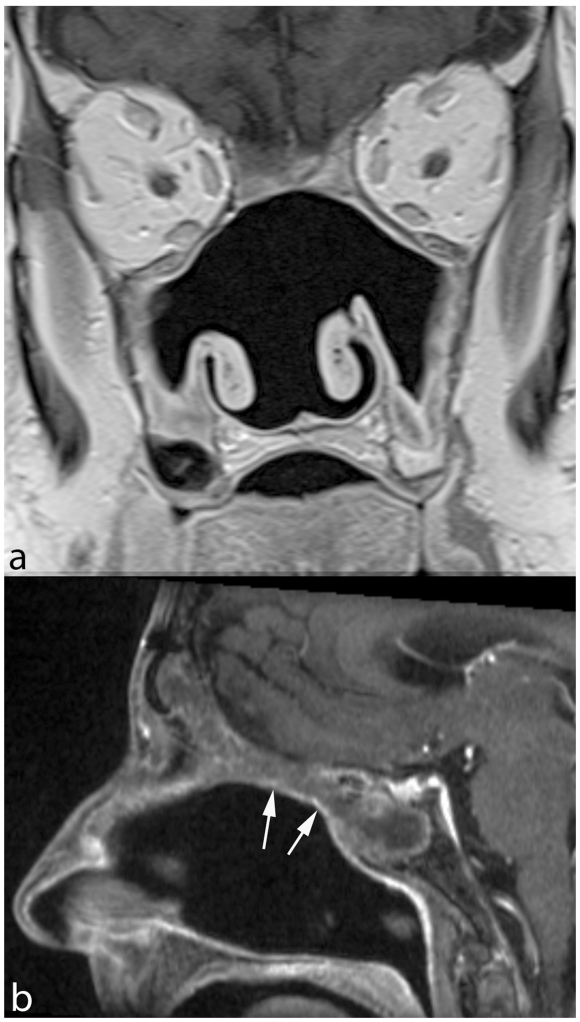

Figure 4 **Craniofacial resection performed with an open surgery approach. The meningogaleal complex exhibits mild and fairly homogeneous contrast enhancement on both SE T1 (a) and fat-saturated GE T1 (b) images, its thickness is regular all along the anteroposterior extension. Reepithelization of the surgical cavity is partially seen (arrows).**

capabilities (and probably beyond the scope) of MRI. More pragmatically, the radiologist should know that, imaged on the sagittal plane, the thickness of the meningogaleal complex/duraplasty is expected to be regular in all its anteroposterior extension (without nodular components) and progressively decreasing during the course of follow-up (Fig. 5). Wide surgical cavities left by extended maxillectomy or orbital exenteration can be filled by muscular flaps, more commonly harvested rotating the temporal muscle. Flaps may enlarge and exhibit bright contrast enhancement as a manifestation of subacute denervation in the early stages of follow-up; identification of the hypointense (on all sequences) aponeurosis along with the striated pattern of muscular fibers invariably allows flaps to be discriminated from recurrent lesions (Fig. 6).

Treatment related inflammatory findings

Thickening of the sinonasal mucosa is quite typical after surgical and radiation treatment. Inflammation manifests as ballooning of the mucosa with hyperintense T2 signal; after contrast application, the epithelial lining enhances, whereas the underlying edematous submucosa does not. After radiation treatment, such changes are immediately seen in the early follow-up studies[20] and may persist for as long as 30 months[21]. Chronic inflammation of the mucosa may also favor the formation of synechiae between bone structures, quite typically between the remnant of the middle turbinate and the lateral nasal wall; mucosal synechiae may provoke sinus blockage and initiate mucocele development. Although the detection on MRI scan of an expanded sinus cavity may raise concerns, careful analysis of sinus drainage pathways as well as signal intensities may clearly discriminate mucoceles from recurrent tumors (Fig. 7). Progressive dehydration (and consequent increase of protein concentration) typically decreases the T2 signal and increases the T1 signal of mucoceles; contrast enhancement within the lesion is absent.

Recurrent lesions

Once a detailed report of treatment applied is provided by the referring clinician, and the radiologist is aware of the related changes on MRI scans, detection of recurrence is significantly facilitated. Recurrent tumors are basically displayed as nodular lesions with variable size. Signal pattern is rarely pathognomonic, because it is extremely variable, and thus a less influential factor. The T2 signal is more typically intermediate, enhancement is generally, although not always, observed. Hyperintensity on b-1000 images and diffusion restriction on the ADC map ($<1 \times 10^{-3}$ mm^2/s) is the general key for the detection of neoplastic lesions on DWI sequences (Fig. 8). Unfortunately, ADC values of recurrent tumors are far from being standardized as the result of the difficulty in collecting large series of data on sinonasal tumors and of the diverse type of sequences and acquisition strategies that can be used in diffusion-weighted imaging. Regarding the site, relapses may be superficial (in which case they are detected at endoscopy first) or located below the mucosa that lines the surgical cavity. When assessing the deep planes, particular attention should be paid to the interfaces between native and reconstructed tissues; any nodule along the otherwise linear profile of the duraplasty/meningogaleal complex, or close to the suture line of a flap, should be considered suspicious until proved otherwise (Figs. 9 and 10). Sometimes the recurrent lesion may be found quite far from the primary tumor site; this is the effect of perineural tumor spread, a pattern of growth characteristic

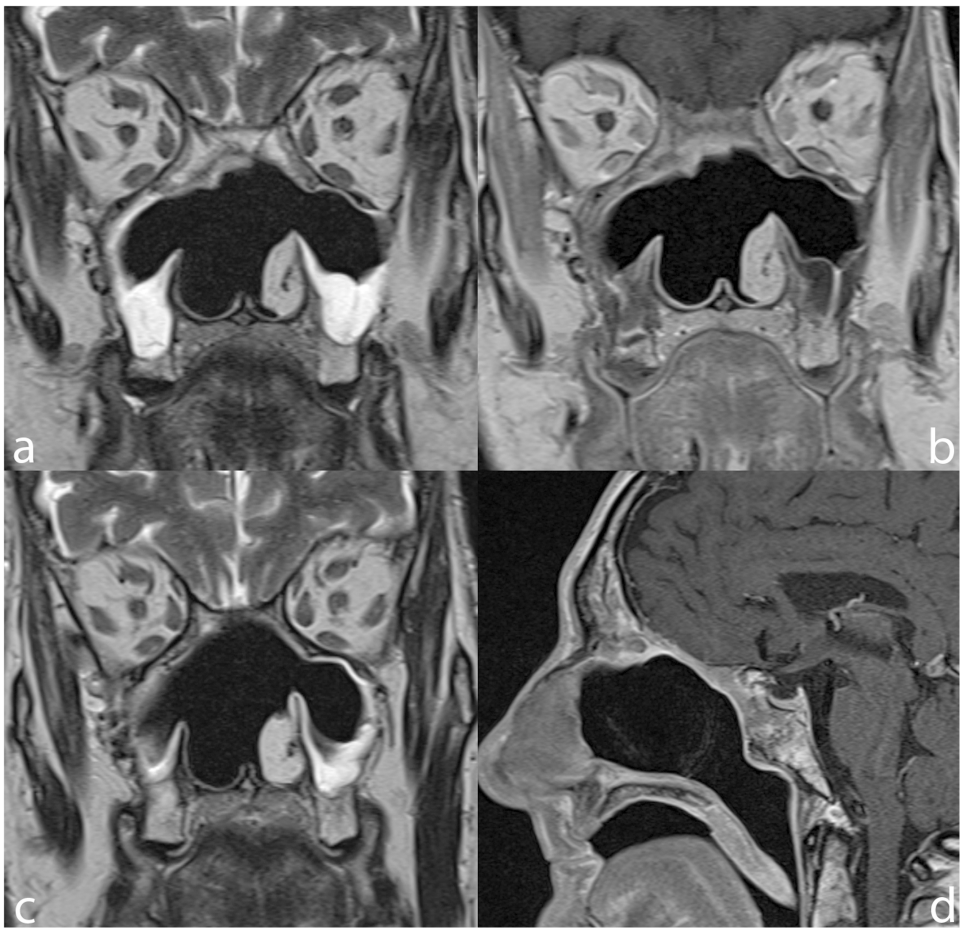

Figure 5 **Craniofacial resection performed with the microendoscopic approach. The comparison between the scans acquired 4 months (a,b) and 20 months (c,d) after surgery demonstrates thinning of the duraplasty and nearly complete regression of mucosal thickenings.**

of adenoid cystic carcinoma, although not infrequently seen also in squamous cell carcinoma and lymphoma. The capability of MRI in depicting such phenomena is unsurpassed: a combination of signs (enlargement and abnormal enhancement of named nerves, remodelling and destruction of foramina and fissures, denervation atrophy of muscles) allows sensitivity and specificity as high as 100% and 85%, respectively[22,23] (Fig. 11). According to a recent paper, MRI technique can be refined with the acquisition of contrast-enhanced constructive interference in steady-state (CISS) sequences, which improves the visualization of nerve abnormalities within the cavernous sinus[24]. Nodal recurrences are seen in up to 13% of patients[4] the incidence being considerably higher in tumors arising from the maxillary sinus[25]; at our institution we tend to survey the neck with ultrasound. On MRI scans particular care should always be paid to retropharyngeal nodes as they are beyond ultrasound field of view. Distant metastases (alone or combined with local and regional recurrence) can be seen in as many as 20% of patients during follow-up[1]. All acquired images should always be carefully scrutinized as metastases may be located in head and neck subsites included in the field of view of the MRI examination (Fig. 12). As a rule of thumb, the first follow-up MRI scan should be scheduled 3 months after the end of treatment, to rule out persistent lesions and provide a baseline for the interpretation of further follow-up examinations. Two basic concepts guide the subsequent plan: most recurrences will occur within 2 years from treatment, thus MRI should be performed every 4 months in this period. Follow-up with imaging should take place for 5 years, however for some histotypes (such as adenoid cystic carcinoma and olfactory neuroblastoma), which may recur later than 5 years after treatment, it should be prolonged to 10 years or longer.

Conclusion

Although challenging, treatment monitoring of paranasal sinus tumors with MRI is a task that can be safely tackled

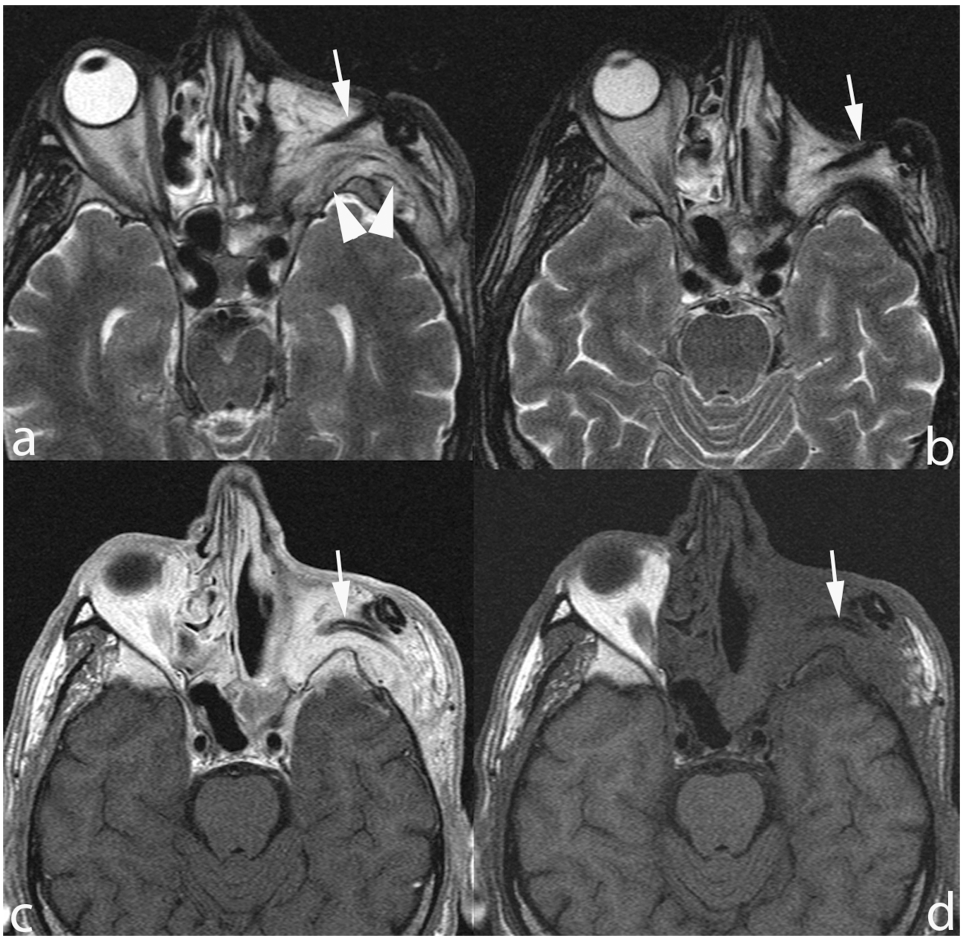

Figure 6 **Radical ethmoidomaxillectomy with orbital exenteration and flap reconstruction. Six months after surgery (a,c,d) the flap shows a hyperintense T2 signal with diffuse and bright enhancement; these findings correspond with subacute denervation, as confirmed by the atrophy demonstrated by the MRI scan performed 12 months after surgery (b). Note the temporalis muscle tendon, rotated in the orbital cavity (arrow) and the striated appearance of muscular fibers (arrowheads), unaltered by edema.**

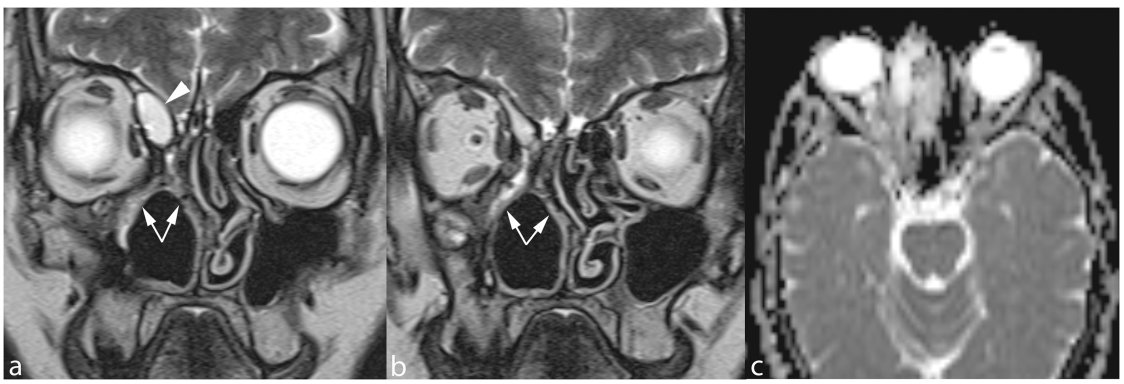

Figure 7 **Radical ethmoidomaxillectomy. Mucosal synechiae (arrows) restrict the residual nasal fossa and obstruct frontal sinus drainage. The small expansile lesion within the lower part of the frontal sinus corresponds to a mucocele (arrowhead) that has developed within a compartmentalized cell. Absence of diffusion restriction on the ADC map (c) confirms the inflammatory nature of the expansile lesion.**

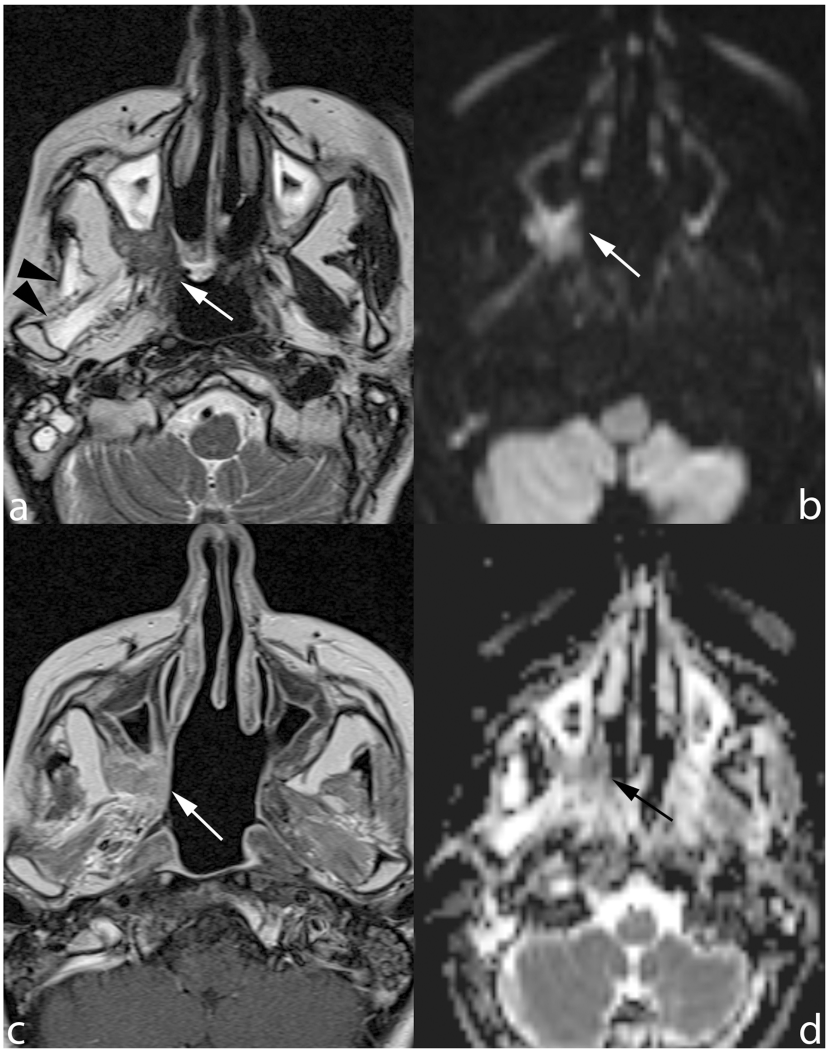

Figure 8 **Radical maxillectomy for adenoid cystic carcinoma. A mass lesion (arrow) is seen in the lowermost part of the pterygopalatine fossa (a,b) exhibiting b-1000 hyperintensity (c) and diffusion restriction (ADC 0.98 × 10^{-3} mm^2/s) (d). Denervation atrophy of masticator muscles (arrowheads) is due to perineural spread reaching the Meckel cave and, antegradely, the mandibular nerve (not displayed in these images).**

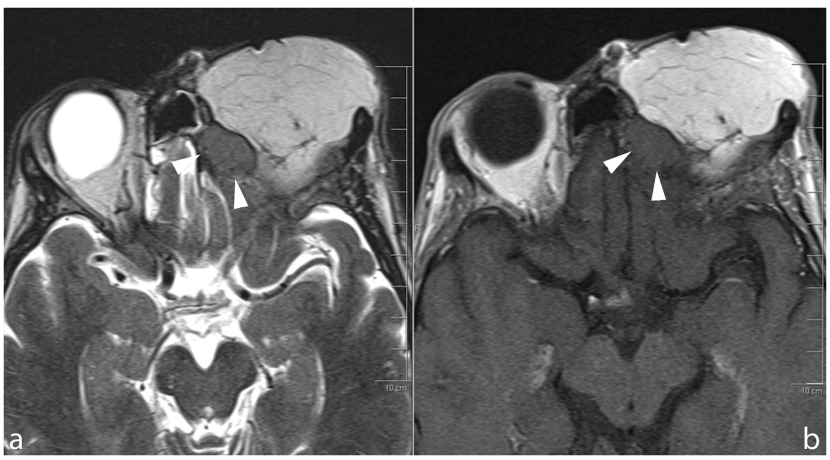

Figure 9 **A nodule is seen at the interface between the flap filling the orbital cavity after exenteration and the skull base in a patient treated for Ewing sarcoma. Although completely unenhancing after contrast application (b), the lesion corresponds to recurrent tumor.**

Figure 10 **Open surgery craniofacial resection. A nodule (arrows) lies beneath the mucosa lining the surgical cavity exhibiting an intermediate T2 signal (a) and mild homogenous enhancement (b). Contact between tumor and dura of the middle cranial fossa is indirectly indicated by thickening and enhancement (arrowheads).**

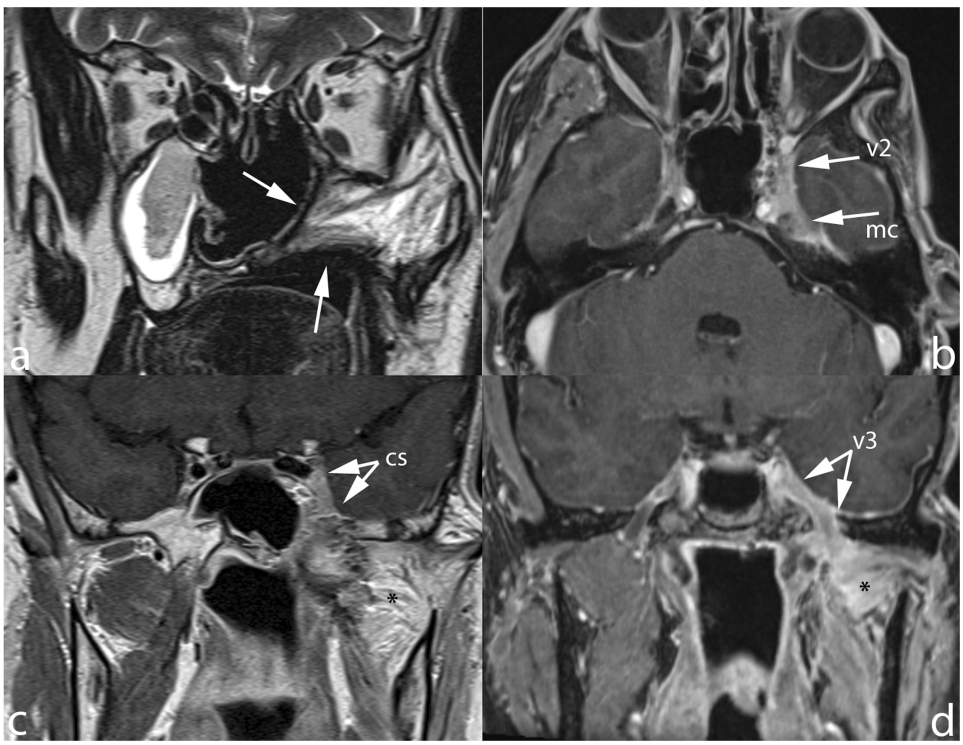

Figure 11 **Radical maxillectomy extended to the hemipalate for squamous cell carcinoma; temporalis muscle flap reconstructs the surgical gap. Perineural recurrent tumor spreading along the maxillary nerve (v2) to reach posteriorly the cavernous sinus (cs) and Meckel cave (mc). Antegrade extension along the mandibular nerve is also seen (v3), the lateral pterygoid muscle (*) shows signs of denervation.**

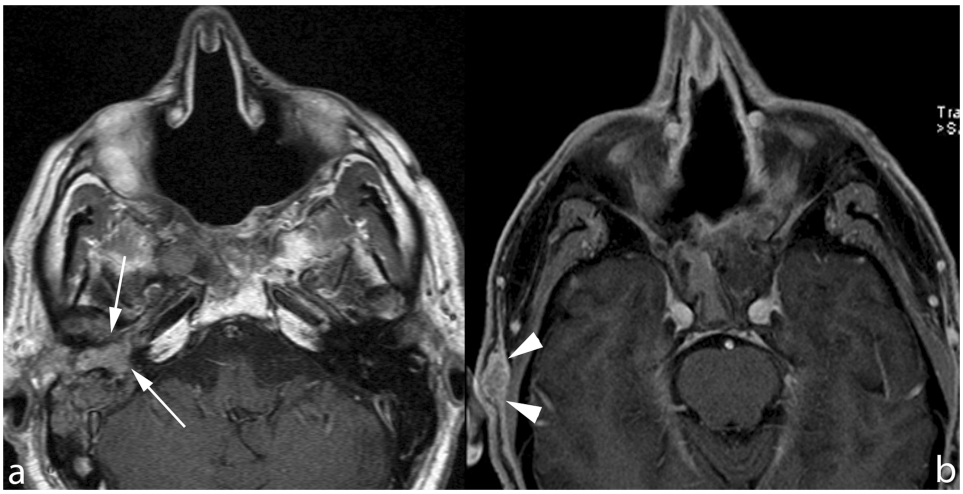

Figure 12 **In two patients treated with craniofacial resection for ethmoid adenocarcinoma, follow-up MRI scans shows metastasis located, respectively, in the middle ear (arrows in (a)) and subcutaneous fat tissue (arrowheads in (b)).**

following a simple checklist: gathering detailed description of treatments applied; being aware of the related expected changes; matching the latter with the findings seen in each individual case; integrating conventional MRI information (T2, T1, fat saturation) with the more sophisticated data provided by DWI and DCE.

References

[1] Khademi B, Moradi A, Hoseini S, Mohammadianpanah M. Malignant neoplasms of the sinonasal tract: report of 71 patients and literature review and analysis. Oral Maxillofac Surg 2009; 13: 191–9. doi:10.1007/s10006-009-0170-8. PMid:19795137.

[2] Sklar EM, Pizarro JA. Sinonasal intestinal-type adenocarcinoma involvement of the paranasal sinuses. AJNR Am J Neuroradiol 2003; 24: 1152–5.

[3] Mendenhall WM, Mendenhall CM, Riggs Jr CE, Villaret DB, Mendenhall NP. Sinonasal undifferentiated carcinoma. Am J Clin Oncol 2006; 29: 27–31. doi:10.1097/01.coc.0000189691.04140.02. PMid:16462499.

[4] Dulguerov P, Jacobsen MS, Allal AS, Lehmann W, Calcaterra T. Nasal and paranasal sinus carcinoma: are we making progress? A series of 220 patients and a systematic review. Cancer 2001; 92: 3012–29. doi:10.1002/1097-0142(20011215)92:12<3012::AID-CNCR10131>3.0.CO;2-E.

[5] Dulguerov P, Allal AS. Nasal and paranasal sinus carcinoma: how can we continue to make progress? Curr Opin Otolaryngol Head Neck Surg 2006; 14: 67–72.

[6] Cantù G, Riccio S, Bimbi G, *et al.* Craniofacial resection for malignant tumours involving the anterior skull base. Eur Arch Otorhinolaryngol 2006; 263: 647–52.

[7] Nicolai P, Battaglia P, Bignami M, *et al.* Endoscopic surgery for malignant tumors of the sinonasal tract and adjacent skull base: a 10-year experience. Am J Rhinol 2008; 22: 308–16. doi:10.2500/ajr.2008.22.3170. PMid:18588765.

[8] Hanna E, DeMonte F, Ibrahim S, Roberts D, Levine N, Kupferman M. Endoscopic resection of sinonasal cancers with and without craniotomy: oncologic results. Arch Otolaryngol Head Neck Surg 2009; 135: 1219–24. doi:10.1001/archoto.2009.173. PMid:20026819.

[9] Batra PS, Luong A, Kanowitz SJ, *et al.* Outcomes of minimally invasive endoscopic resection of anterior skull base neoplasms. Laryngoscope 2010; 120: 9–16.

[10] Zimmer LA, Theodosopoulos PV. Anterior skull base surgery: open versus endoscopic. Curr Opin Otolaryngol Head Neck Surg 2009; 17: 75–8.

[11] Chang DW, Langstein HN, Gupta A, *et al.* Reconstructive management of cranial base defects after tumor ablation. Plast Reconstr Surg 2001; 107: 1346–55. doi:10.1097/00006534-200105000-00003. PMid:11335798.

[12] Resto VA, Deschler DG. Sinonasal malignancies. Otolaryngol Clin North Am 2004; 37: 473–87. doi:10.1016/S0030-6665(03)00159-2.

[13] Tofts PS, Brix G, Buckley DL, *et al.* Estimating kinetic parameters from dynamic contrast-enhanced T(1)-weighted MRI of a diffusable tracer: standardized quantities and symbols. J Magn Reson Imaging 1999; 10: 223–32. doi:10.1002/(SICI)1522-2586(199909)10:3<223::AID-JMRI2>3.0.CO;2-S.

[14] Baba Y, Furusawa M, Murakami R, *et al.* Role of dynamic MRI in the evaluation of head and neck cancers trated with radiation therapy. Int J Radiat Oncol Biol Phys 1997; 37: 783–7.

[15] Semiz Oysu A, Ayanoglu E, Kodalli N, Oysu C, Uneri C, Erzen C. Dynamic contrast-enhanced MRI in the differentiation of posttreatment fibrosis from recurrent carcinoma of the head and neck. Clin Imaging 2005; 29: 307–12. doi:10.1016/j.clinimag.2005.01.024. PMid:16153535.

[16] Kim S, Loevner LA, Quon H, *et al.* Prediction of response to chemoradiation therapy in squamous cell carcinomas of the head and neck using dynamic contrast-enhanced MR Imaging. AJNR Am J Neuroradiol 2010; 31: 262–8. doi:10.3174/ajnr.A1817. PMid:19797785.

[17] De Foer B, Vercruysse JP, Pilet B, *et al.* Single-shot, turbo spin-echo, diffusion-weighted imaging versus spin-echo-planar, diffusion- weighted imaging in the detection of acquired middle ear cholesteatoma. AJNR Am J Neuroradiol 2006; 27: 1480–2.

[18] Abdel Razek AAK, Kandeel AY, Soliman N, *et al.* Role of diffusion-weighted echo-planar MR imaging in differentiation of residual or recurrent head and neck tumors and posttreatment changes. AJNR Am J Neuroradiol 2007; 28: 1146–52. doi:10.3174/ajnr.A0491. PMid:17569975.

[19] Draf W. Endonasal microendoscopic frontal sinus surgery, the Fulda concept. Op Tech Otolaryngol Head Neck Surg 1991; 2: 234–40. doi:10.1016/S1043-1810(10)80087-9.

[20] Wang JH, Lee BJ, Lee JH, Kim IJ, Jang YJ. Development of mucosal thickening after radiotherapy in contralateral sinuses of patients with nasal cavity and/or paranasal sinus carcinoma. Ann Otol Rhinol Laryngol 2008; 117: 844–8.

[21] Raviv J, Downing L, Le QT, Hwang P. Radiographic assessment of the sinuses in patients treated for nasopharyngeal carcinoma. Am J Rhinol 2008; 22: 64–7. doi:10.2500/ajr.2007.21.3091. PMid:17958946.

[22] Maroldi R, Farina D, Borghesi A, Marconi A, Gatti E. Perineural tumor spread. Neuroimaging Clin N Am 2008; 18: 413–29. doi:10.1016/j.nic.2008.01.001. PMid:18466839.

[23] Hanna E, Vural E, Prokopakis E, Carrau R, Snyderman C, Weissman J. The sensitivity and specificity of high-resolution imaging in evaluating perineural spread of adenoid cystic carcinoma to the skull base. Arch Otolaryngol Head Neck Surg 2007; 133: 541–5. doi:10.1001/archotol.133.6.541. PMid: 17576903.

[24] Yagi A, Sato N, Takahashi A, *et al.* Added value of contrast-enhanced CISS imaging in relation to conventional MR images for the evaluation of intracavernous cranial nerve lesions. Neuroradiology 2010 Apr 10 [E-pub ahead of print].

[25] Cantù G, Bimbi G, Miceli R, *et al.* Lymph node metastases in malignant tumors of the paranasal sinuses: prognostic value and treatment. Arch Otolaryngol Head Neck Surg 2008; 134: 170–7.